RESEARCH OUTPUTS / RÉSULTATS DE RECHERCHE

Study of Cr-N bonding in nitrided stainless steel coatings by low-energy electron induced X-ray spectroscopy (LEEIXS)

Colaux, Julie; Terwagne, Guy

Published in:
Journal of Electron Spectroscopy and Related Phenomena

Publication date:
2003

Document Version
Peer reviewed version

Citation for pulished version (HARVARD):
Colaux, J & Terwagne, G 2003, 'Study of Cr-N bonding in nitrided stainless steel coatings by low-energy electron induced X-ray spectroscopy (LEEIXS)', *Journal of Electron Spectroscopy and Related Phenomena*, vol. 133, pp. 17-25.

Study of Cr–N bonding in nitrided stainless steel coatings by low-energy electron induced X-ray spectroscopy (LEEIXS)

J. Colaux*, G. Terwagne

*Laboratoire d'Analyses par Réactions Nucléaires, Facultés Universitaires Notre-Dame de la Paix,
61 rue de Bruxelles-B-5000, Namur, Belgium*

Abstract

Thin nitrided stainless steel coatings (400–500 nm) were deposited onto polished low carbon steel substrates by magnetron sputtering in a reactive atmosphere of argon–nitrogen mixture. A series of coatings were deposited with a total gas-flow constant while increasing nitrogen proportion. The nitrogen content which was determined by nuclear reaction analysis (NRA) was found to increase with increasing N_2 flow-rate. The chemical bond between chromium and nitrogen was controlled by low-energy electron induced X-ray spectroscopy (LEEIXS) with a wavelength dispersive spectrometer equipped with a TlAP crystal ($2d = 2.576$ nm). The low-energy sub-band generated by the bonding between chromium and nitrogen allow us to determine the proportion of nitrogen contained in the coatings.
© 2003 Elsevier B.V. All rights reserved.

1. Introduction

Austenitic stainless steels are well known for their corrosion resistant properties but their performance is limited by their poor wear resistance. Nitriding of these steels can be performed by several techniques, such as conventional ion implantation [1–6], pulsed plasma nitriding [7] and plasma immersion ion implantation (PI³) [8]. However, when chromium nitrides are formed they affect the corrosion resistance of stainless steel. One crucial experimental point to prevent chromium nitride (CrN) clusters formation is to keep the temperature below a critical value of approximately 450 °C [9]. At low temperatures below 400 °C, nitrogen remains in solid solution, producing a phase that has been variously called 'S-phase' [9], 'expanded austenite' [10], γ_N-phase [4–6], M or ε'-phase [11,12].

The aim of the present investigation is to study the chemical bonding between chromium and nitrogen present within the structure of nitrided stainless steel coatings by means of low-energy electron induced X-ray spectroscopy (LEEIXS).

* Corresponding author. Tel.: +32-81-72-54-78;
fax: +32-81-72-54-74.
E-mail address: julie.colaux@fundp.ac.be (J. Colaux).

2. Sample preparation

The coatings were deposited using an unbalanced DC-magnetron sputtering system placed in a small chamber of $0.05\,m^3$ equipped with a 400 l/s turbo-molecular pump which provided a base pressure of 10^{-5} Pa. A 50 mm diameter AISI 304L (composition in wt.%—C: 0.03%, Mn: 2%, Si: 1%, P: 0.045%, S: 0.03%, Cr: 18–19%, Ni: 8–12%, Fe: balance) disk target was placed just above the magnets with a good thermal contact to the holder in order to cool the magnetic material with water during deposition. The source to sample holder distance was 150 mm and a chimney was placed between the target and the substrate to prevent contamination of the whole chamber and to confine the plasma in order to reproduce more easily deposition conditions. A shutter was placed between the top of the chimney and the sample holder in order to avoid deposition during target cleaning for 5 min before each deposition.

Steel substrates were cut into $20\,mm \times 20\,mm$ coupons and were polished in order to create an abrupt interface between the coating and the substrate. Polishing was realized using SiC papers with a grit ranging between 180 and 1200. The substrates were then polished with diamond paste of $9\,\mu m$. Finally, they were cleaned in an ultrasonic bath with pentane before loading into the chamber. Prior each deposition, the steel substrate (which was grounded) was etched in order to remove oxides from the steel surface and to enhance coating adhesion.

Depositions were made at room temperature using a magnetron with power fixed at $10.2\,W/cm^2$. The coatings were reactively deposited for 40 and 60 min with various Ar/N_2 gas mixtures, which gave thickness between 1.25 and $1.56\,\mu m$ (Table 1). The proportion of N_2 in the sputter gas was varied by changing the N_2 flow-rate and compensating the Ar flow-rate, such that the total gas-flow-rate remained constant at 35 sccm. These flows correspond to a total pressure of 0.2–0.3 Pa measured with a Baratron gauge placed in the deposition chamber. The deposition parameters are given in Table 1.

3. Fundamentals and experimental

The fundamentals of the LEEIX spectroscopy can be found in [13–20]. This spectroscopy is based on the ionization of the inner shell of the element under investigation by electrons of a few keV. Characteristics X-rays emitted by the sample have wavelengths in the order of 0.2–10 nm. X-rays in this range are called soft X-rays. The advantage of studying L band of elements of the first series of transition elements (or K_α band of light elements [21]) is that the phenomenon implies valence electrons which participate directly to chemical bond [22–25]. Electronic transitions that take place from valence bands to inner shell show thus clear chemical effects. In the present work, the difference could be established between chromium bond to stainless steel components (Fe, Ni and Mn) and chromium bond to nitrogen in nitrided stainless steel coatings.

The X-ray emission instrument used in this study is a wavelength dispersive X-ray spectrometer. A schematic diagram of the experimental set-up which is pumped with a primary rotary pump is shown in Fig. 1. The excitation source is a DC glow-discharge electron gun with an aluminum cathode. The electron beam escapes from the source through a circular aperture in the anode and strikes the surface of the sample under investigation. Characteristics X-rays emitted by this latter are then collimated by a Soller slits system which defines a parallel X-rays beam dispersed by a flat analyzing crystal and finally detected by a gas-flow proportional counter filled with an Ar/CH_4 (90%/10%) mixture.

The energy of the incident electron beam is chosen to be approximately 4 keV in order to increase the analyzed sample depth from which characteristic X-rays are emitted and analyzed and thus to increase the sensitivity of the analysis. The gas discharge pressure is 25 Pa and the current density $5\,\mu A/mm^2$. The spec-

Table 1
Deposition parameters ($P = 10.2\,W/cm^2$ and $p = 0.2$–0.3 Pa) and atomic fraction of nitrogen

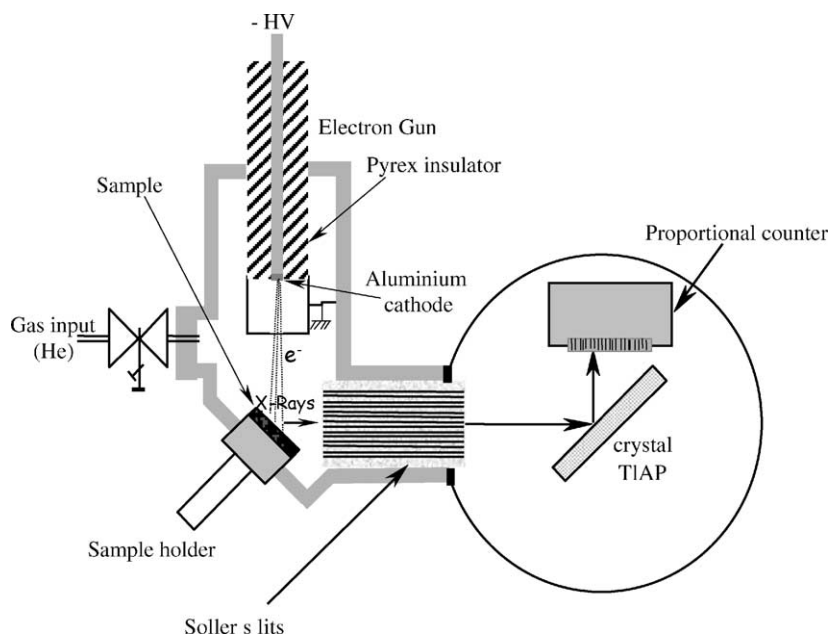| t_{dep} (min)	Thickness (μm)	N_2 flow-rate (sccm)	[N] (at.%)
40	1.28	0.0	0.3
40	1.39	3.0	9.0
60	1.56	6.0	17.0
60	1.56	8.0	16.5
60	1.41	12.0	21.0
60	1.25	13.0	24.0

Fig. 1. Schematic diagram of the LEEIXS spectrometer.

trometer scans 2θ angles between $107°$ and $122°$ by steps of $0.15°$.

In order to detect chromium L radiations, namely $L_{\alpha1-2}$ ($E = 574.1 - 2.3 = 571.8$ eV, $\lambda = 2.17$ nm) and L_β ($E = 583.8 - 2.3 = 581.5$ eV, $\lambda = 2.13$ nm) [26] with the best possible resolution, we have chosen a thallium acid phthalate (TlAP) crystal with a $2d$ parameter just above 2.17 nm. Indeed, this dispersive device has a $2d$ parameter of 2.576 nm which provides a good energy resolution and has a very high reflective factor for low-energy X-rays.

4. Results and discussion

4.1. Simulation of experimental spectra

Experimental spectra were deconvoluated by adjusting lorentzian peaks and varying parameters like position, width and area of these peaks. Lorentz peaks were fitted, with parameters corresponding in a first time to values found in the literature (see below). Then, parameters were adjusted in such a way that an optimum agreement with the recorded spectrum is achieved. Special attention was required, since an op-

timum agreement between the calculated and the experimental spectra does not necessarily lead to a physically correct interpretation of the spectra.

As explained above, the aim of this work was to determine the presence of chromium nitrides in the different nitrided coatings, which contain increasing nitrogen concentrations. Nuclear reaction analysis (NRA) with the $^{14}N(d, p)^{15}N$ nuclear reaction at $E_d = 1.1$ MeV has been performed on these coatings in order to precisely determine the atomic fraction of nitrogen (The quantification of nitrogen by the nuclear reaction $^{14}N(\alpha, p)^{17}O$ is given in Terwagne et al. [27]). The results are also listed in Table 1 where the nitrogen atomic fraction is reported versus nitrogen flow-rate injected in the deposition chamber.

4.2. Standards

The first step of this study was to realize a library of standards containing chromium in different valence states, such as metallic chromium, stainless steel AISI 304L and chromium nitride. The chromium standard was a Goodfellow foil (thickness: 0.5 mm, purity 99.7%) whereas the iron standard was a foil from Advent Research Materials Ltd. (thickness 0.25 mm,
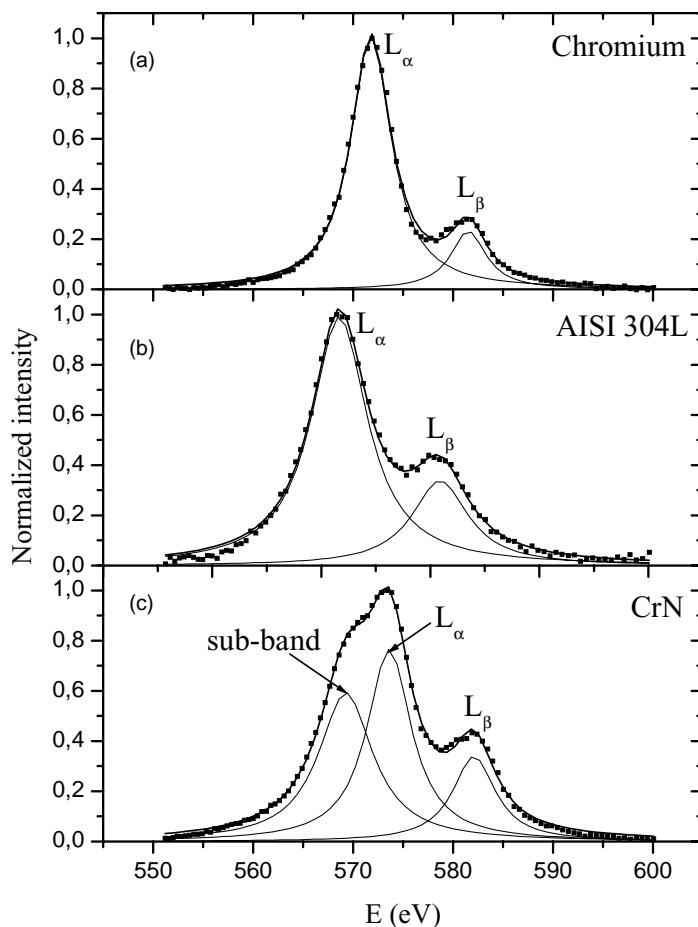
Fig. 2. L X-ray experimental spectra obtained on standard samples: (a) chromium, (b) stainless steel, (c) CrN, bombarded with 4 keV electron beam.

purity 99.5%). The CrN standard was a PVD layer deposited on steel and analyzed by nuclear reaction analysis and particules-induced X-ray emission (PIXE) at LARN to check the stoichiometry.

Experimental spectra of the chromium standards are shown in Fig. 2. We observe only two peaks in the pure chromium spectrum which correspond to the two main transitions L_α and L_β. The energy gap between these two bands is 9.74 eV which is in excellent agreement with Pappert et al. [14], as they give a gap of 9.78 eV. Moreover, Table 2 gives the chemical shift between pure chromium and stainless steel which is +0.13 eV for L_α band.

In the case of L X-ray spectra of chromium contained in partially ionic compounds, such as nitrides,

it is supposed that, as in the case of the L spectra of vanadium and titanium [23–25], three main energy transitions (peaks) are responsible for the shape of the overall spectrum of chromium compounds. Their formation can be explained on the basis of the Ligand Field Theory [28] which is an application of Molecular Orbitals Theory. Each spectral feature is then explained from an electron transition between a specific Molecular Orbital and an inner level in relation to the normal dipole selection rules [29]. CrN crystallizes with an NaCl lattice in which the metallic chromium ion is in an octahedral environment of non-metals, namely the N atoms. The components L_α and L_β then involve $2t_{2g}$ orbitals while the sub-band that appears at low energy is associated with $2e_g$ orbital. Examination

Table 2
Experimental parameters obtained with electrons of 4 keV bombarding standard samples

	Cr	AISI 304L	CrN
Max L_α (eV)	571.79 ± 0.02	571.66 ± 0.03	573.62 ± 0.05
Half width (eV)	4.91 ± 0.06	6.25 ± 0.09	5.37 ± 0.17
Area L_α	7.77 ± 0.07	9.72 ± 0.13	6.46 ± 0.33
Max L_β (eV)	581.53 ± 0.08	580.89 ± 0.09	582.09 ± 0.06
Half width (eV)	4.29 ± 0.24	6.28 ± 0.29	5.17 ± 0.19
Area L_β	1.56 ± 0.07	3.33 ± 0.13	2.75 ± 0.09
Max sub-band (eV)	–	–	569.27 ± 0.09
Half width (eV)	–	–	6.60 ± 0.17
Area sub-band	–	–	6.14 ± 0.31

of the spectrum of CrN shows that peaks L_α and L_β are shifted towards high energy side with respect of pure chromium. Similar phenomenon has been observed for chromium nitrides by Gaillard and Romand [30]. For CrN, they give a shift of the L_α peak as high as 4.27 eV. In the present investigation, L_α peak is shifted by 1.83 eV towards higher energies.

4.3. Nitrided stainless steel coatings

The second step of the present investigation was to analyze the nitrided stainless steel coatings by exactly the same procedure. X-ray and electron diffraction analysis [31] of these coatings show that the structure formed is an expanded face-centered cubic array constituted of stainless steel components with nitrogen present at interstitial sites. There is no chromium nitride precipitation as we do not observe any XRD signal typical of CrN. Moreover, electron diffraction patterns do not show any spot or ring consistent with chromium nitride. However, as the enthalpy of formation of CrN is high compared with other possible nitride compounds in stainless steel, there must be some Cr–N bonds but they are localized in the fcc array. This is consistent with the deposition method as coatings are formed by sputtering deposition at room temperature. The growing temperature is thus insufficient to allow the diffusion of chromium to form CrN precipitate. Experimental LEEIXS spectra of nitrided stainless steel are composed of some chromium bond to components of the stainless steel and of chromium bond to nitrogen present in the coating. As previously explained, $L_{\alpha,\beta}$ spectrum of chromium will generate two and three peaks, respectively. However, experimental pa-

rameters obtained with standards can not be used to fit spectra of nitrided stainless steel coatings as peak parameters are influenced by the hybridization of Cr and N orbitals which is different in each coating analyzed. Moreover, the self-absorption is different for each peak and dependent of the composition of the sample. The ratio of the areas L_α/L_β of CrN cannot thus be taken to fit L_α and L_β band of chromium bond to nitrogen in stainless steel. These reasons explain the fitting procedure chosen to analyze nitrided stainless steel coatings. Only three bands will be fitted. The first one, labeled L_α contains contributions from Cr atoms bond to stainless steel components (Fe, Ni and Mn) and from Cr atoms bond to N L_β contains also the two equivalent contributions. However, the low-energy sub-band is only due to Cr bond to nitrogen in the steel. That band will thus be used to quantify the Cr–N bonding.

By keeping the energy of the electron beam constant at 4 keV we know that the analyzed thickness (calculated by Brown [32]) is similar (120 nm) for all coatings. Some experimental spectra (for films containing 0.3, 9.0, 17.0 and 24.0 at.%) are presented in Fig. 3a–d in order to show the evolution of the low-energy sub-band versus nitrogen content of the film. It is evident that this low-energy band increases with nitrogen content. Table 3 displays the parameters of the three bands for lower and higher nitrogen content, respectively. From those tables, the evolution of some parameters are plotted in Figs. 4–6. As previously observed [30], the position of the L_α band is shifted towards higher energies as the bonding between nitrogen and chromium increases. This is clearly highlighted in Fig. 4. As the nitrogen fraction increases, the interaction between Cr 3d and ligand
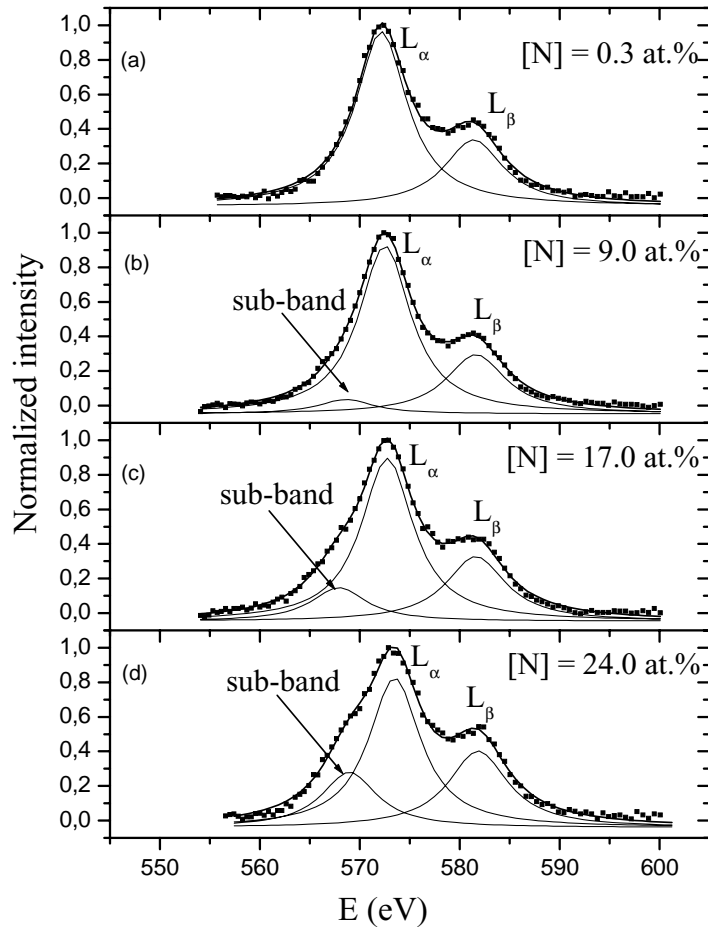
Fig. 3. Fitting of L X-ray experimental spectra obtained with 4 keV electron beam.

2p orbitals increases also to form $2e_g$, $1t_{2g}$, $2t_{2g}$ and $3e_g$ Molecular Orbitals levels. The probability to observe transitions which give rise to L_β band is thus increased as shown in Fig. 5.

Finally, Fig. 6 plots the area of the low-energy sub-band which is directly related to the nitrogen content. As chromium nitrides formation enthalpy is higher [33] compared with possible nitrides of other

Table 3
Experimental parameters obtained on coatings with an electron beam of 4 keV

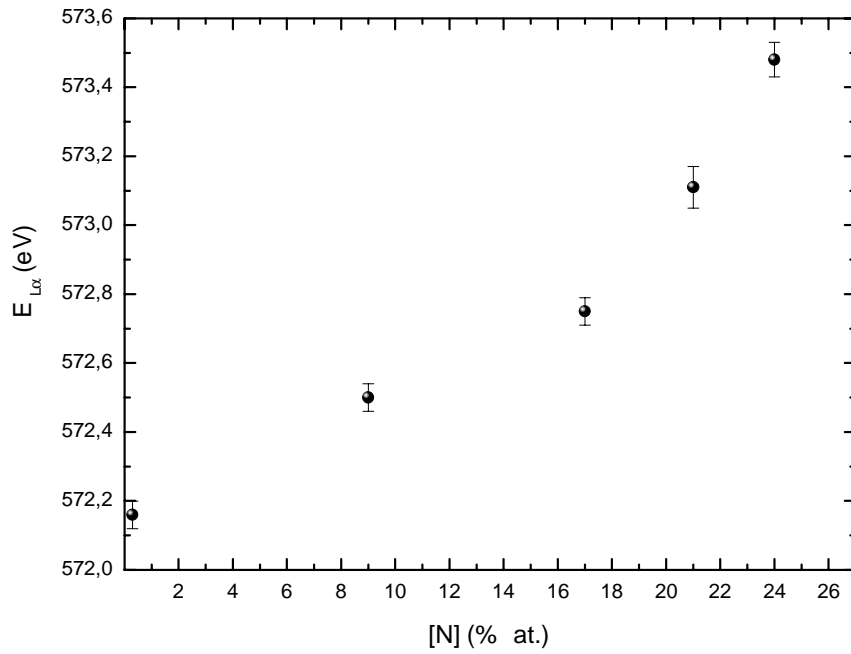|	[N] (at.%)				
	0.3	9.0	17.0	21.0	24.0
L_α (eV)	572.1 ± 0.04	572.50 ± 0.04	572.75 ± 0.04	573.11 ± 0.06	573.48 ± 0.05
Area L_α	9.97 ± 0.19	9.61 ± 0.15	9.32 ± 0.17	9.02 ± 0.17	8.56 ± 0.18
L_β (eV)	581.39 ± 0.11	581.63 ± 0.07	581.63 ± 0.08	581.61 ± 0.09	581.85 ± 0.09
Area L_β	4.35 ± 0.22	3.89 ± 0.07	4.25 ± 0.08	4.80 ± 0.12	5.02 ± 0.11
Sub-band (eV)	–	568.63 ± 0.05	567.91 ± 0.24	568.43 ± 0.22	568.95 ± 0.17
Area sub-band	–	0.87 ± 0.15	2.04 ± 0.06	2.55 ± 0.18	3.37 ± 0.18

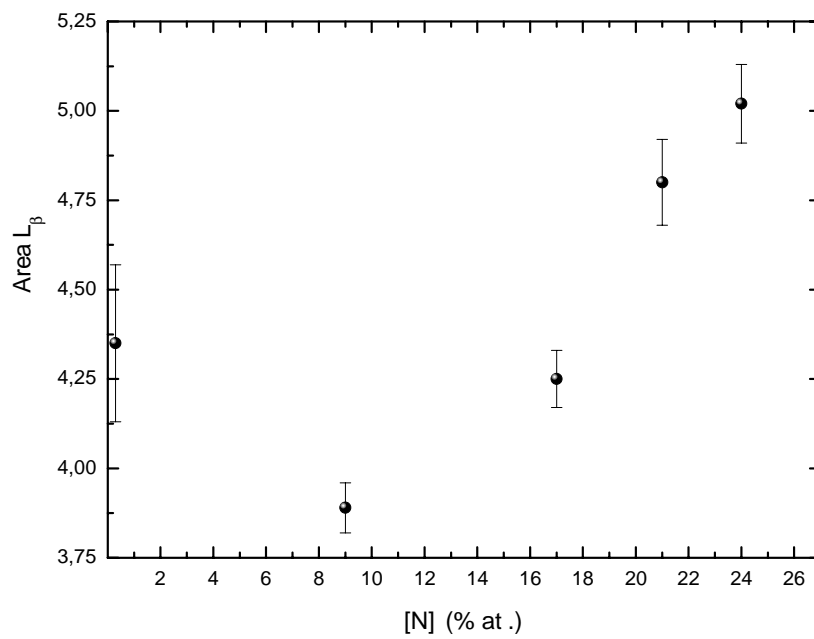Fig. 4. L_α energy vs. nitrogen atomic concentration of analyzed coatings.

Fig. 5. Area of L_β peak vs. nitrogen atomic concentration of analyzed coatings.
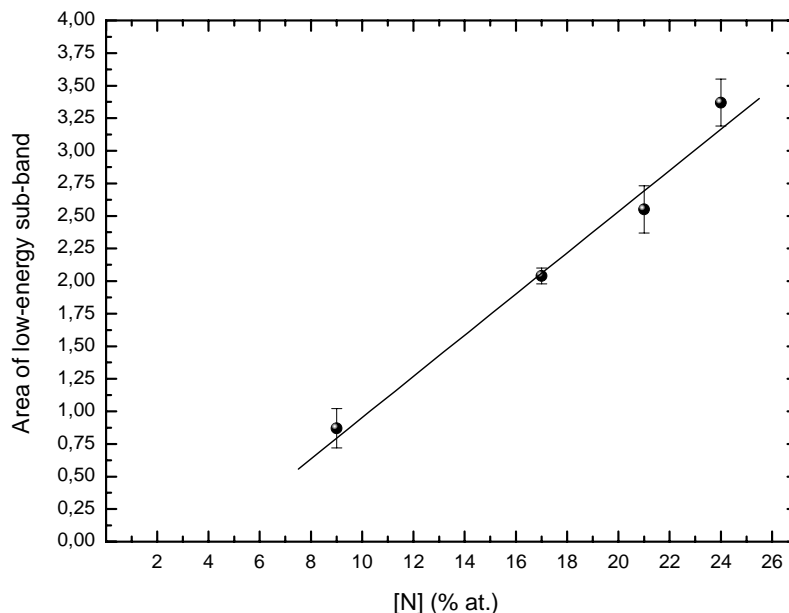
Fig. 6. Area of the low-energy sub-band vs. nitrogen atomic concentration of analyzed coatings.

elements (mainly Fe_xN), during the sputtering phase, nitrogen reacts preferentially with chromium atoms. This is the reason why a small shoulder is seen in the LEEIX spectrum as soon as the coating contains nitrogen. This effect is caused by the interaction between Cr 3d and ligand N 2p orbitals as explained previously.

5. Conclusion

This paper has shown the effectiveness of LEEIX spectroscopy to study Cr–N bonding. In case of complicated compounds like (Fe–Cr–Ni)N, as obtained by nitriding of stainless steel, we have shown the correlation between low-energy sub-band area and nitrogen content measured by nuclear reaction analysis. Moreover, the present work has allowed us to confirm the assumption of nitrogen localized at interstitial position and forming localized Cr–N bonds but without forming precipitates of CrN that would be observed by X-ray and electron diffraction. The corrosion resistance of the analyzed nitrided stainless steel coatings is thus probably unaffected compared to original stainless steel. To our knowledge, Cr–N bonding could

only be detected with XPS spectroscopy. However, XPS would give an information from some nanometers for stainless steel coatings, whereas in LEEIXS an electron beam of 4 keV analyzes a thickness of some 120 nm. Moreover, LEEIXS can easily be installed in a research laboratory in regards with XPS that requires expensive apparatus due to ultra-high vacuum necessary to such a technique. Finally, LEEIXS could also be used to determine the content of nitrogen or oxygen of binary compounds, such as Cr_xN_y, Cr_xO_y, ... This easy characterization could be very useful to materials research sections non-equipped with nuclear analysis facilities.

Acknowledgements

References

[1] G. Wagner, T. Louis, R. Leutenecker, U. Gonser, Hyperfine Interact. 46 (1989) 501.

[2] D.L. Williamson, O. Orturk, S. Glich, R. Wei, P.J. Wilbur, Nucl. Instrum. Methods B59–B60 (1991) 737.

[3] Th. Briglia, G. Terwagne, F. Bodart, C. Qwaeyhaegens, J. D'Haen, L.M. Stals, Surf. Coat. Technol. 80 (1996) 105.

[4] D.L. Williamson, J.A. Davies, P.J. Wilbur, Surf. Coat. Technol. 103–104 (1998) 178.

[5] R. Wei, Surf. Coat. Technol. 83 (1996) 218.

[6] O. Oztürk, D.L. Williamson, J. Appl. Phys. 77 (1995) 3839.

[7] E. Menthe, K.T. Rie, J.W. Schultze, S. Simon, Surf. Coat. Technol. 74–75 (1995) 412.

[8] G.A. Collins, R. Hutchings, J. Tendys, Mater. Sci. Eng. A139 (1991) 135.

[9] Z.L. Zhang, T. Bell, Surf. Eng. 1 (1985) 131.

[10] C. Blawert, H. Kalvelage, B.L. Mordike, G.A. Collins, K.T. Short, Y. Jiraskova, O. Schneeweiss, Surf. Coat. Technol. 136 (2001) 181.

[11] K. Marchev, C.V. Cooper, J.T. Blucher, B.C. Giessen, Surf. Coat. Technol. 99 (1998) 225.

[12] K. Marchev, R. Hidalgo, M. Landis, R. Vallerio, C.V. Cooper, B.C. Giessen, Surf. Coat. Technol. 112 (1999) 67.

[13] C.J. Powell, Rev. Modern Phys. 48 (1) (1976) 33–47.

[14] E. Pappert, J. Flock, J.A.C. Broekaert, Spectrochim. Acta, Part B 54 (1999) 299.

[15] J. Geyger, J. Reisel, J. Flock, J.A.C. Broekaert, Spectrochim. Acta, Part B 55 (2000) 49.

[16] M. Romand, F. Gaillard, M. Charbonnier, Plasma Surface Engineering, vol. 2, DGM Information Gesellschaft Verlag, Oberursel, 1989, p. 759.

[17] M.J. Romand, F. Gaillard, M. Charbonnier, Adv. X-Ray Anal. 35 (1992) 767.

[18] M. Romand, M. Charbonnier, J. Baborowski, J. Physique IV (France) 6 (1996) C4-467.

[19] D.S. Urch, L.N. Mazalov, Chemistry in Britain, Royal Society Chemistry London, October 1994, p. 832.

[20] M. Romand, R. Bador, M. Charbonnier, F. Gaillard, X-Ray Spectrom. 16 (1987) 7.

[21] A.K. Gyani, P. McClusky, D.S. Urch, M. Charbonnier, F. Gaillard, M. Romand, Adv. X-Ray Anal. 33 (1990) 247.

[22] S. Shin, M. Fujisawa, H. Ishii, Y. Harada, M. Watanabe, M.M. Grush, T.A. Callcott, R.C.C. Perera, E.Z. Kurmaev, A. Moewes, R. Winarski, S. Stadler, D.L. Ederer, J. Electron Spectrosc. Relat. Phenom. 92 (1998) 197.

[23] D.W. Fischer, J. Appl. Phys. 39 (10) (1968) 4757.

[24] D.W. Fischer, Adv. X-Ray Anal. 13 (1969) 159.

[25] D.W. Fischer, J. Appl. Phys. 40 (10) (1969) 4151.

[26] J.A. Bearden, A.F. Burr, Rev. Mod. Phys. 39 (1967) 125.

[27] G. Terwagne, J. Colaux, G.A. Collins, F. Bodart, Thin Solid Films 377–378 (2000) 441.

[28] D.F. Shriver, P.W. Atkins, Inorganic Chemistry, third ed., Oxford University Press, Oxford, 1999.

[29] D.W. Fischer, J. Appl. Phys. 41 (9) (1970) 3561.

[30] F. Gaillard, M. Romand, Surf. Interface Anal. 16 (1990) 429.

[31] J. Colaux, D.R.G. Mitchell, K.T. Short, G.A. Collins, G. Terwagne, submitted for publication.

[32] D.B. Brown, in: J.W. Robinson (Ed.), Handbook of Spectroscopy, vol. I, CRC Press, Boca Raton, 1979, p. 249.

[33] Handbook of Chemistry and Physics, vol. D-61, 55th ed., CRC Press, Boca Raton, 1974/1975.